An Optimal Power-Throughput Tradeoff Study for MIMO Fading Ad-Hoc Networks

Homayoun Yousefi'zadeh and Hamid Jafarkhani

(Invited Paper)

Abstract: **In this paper, we study optimal tradeoffs of achievable throughput versus consumed power in wireless ad-hoc networks formed by a collection of multiple antenna nodes. Relying on adaptive modulation and/or dynamic channel coding rate allocation techniques for multiple antenna systems, we examine the maximization of throughput under power constraints as well as the minimization of transmission power under throughput constraints. In our examination, we also consider the impacts of enforcing quality of service requirements expressed in the form of channel coding block loss constraints. In order to properly model temporally correlated loss observed in fading wireless channels, we propose the use of finite-state Markov chains. Details of fading statistics of signal-to-interference-noise ratio, an important indicator of transmission quality, are presented. Further, we objectively inspect complexity versus accuracy tradeoff of solving our proposed optimization problems at a global as oppose to a local topology level. Our numerical simulations profile and compare the performance of a variety of scenarios for a number of sample network topologies.**

Index Terms: **Fading wireless ad-hoc networks, markov chain, multiple antenna, power minimization, quality of service (QoS), Rayleigh channel, Rician channel, throughput maximization.**

I. INTRODUCTION

Recent proliferation of wireless devices has greatly facilitated access and exchange of information. Ad-hoc networks are a special class of wireless networks where there is no such fixed infrastructure as base stations for allocating channels, controlling usage, or provisioning of services. Rather, they need to be adaptively self-organizing. Any node in an ad-hoc network can transmit, receive, or relay signals. While exploiting the advantages of wireless ad-hoc networks, designers are facing tremendous challenges.

Optimal allocation of resources under the power constraint is critical for providing the desired level of quality of service (QoS), efficient utilization of the limited wireless spectrum, and longer battery life of the mobile devices. Due to the openness of transmission media, communication over a wireless link is prone to interferences from other links in addition to noise. While increasing the transmission power of a user in an ad-hoc network will make the outgoing link more reliable, it also shortens battery life and causes interference to other users. The observed signal-to-interference-noise ratio (SINR) at the receiver is introduced to capture the quality of received signal. Further, considering the mobility of the nodes and fading effects in an ad-hoc network, links are subject to the Doppler spread and temporally correlated loss. The 2-state Gilbert-Elliott model [1], [2] and its extensions [3]–[5] have been widely used as Markov chain modeling tools of fading channels.

Multiple antenna systems substantially reduce the effect of multipath fading in the wireless channels through antenna diversity. Transmit antenna diversity in the form of space-time block codes (STBCs) of [6] and [7] has been adopted in many recent wireless standards. Receive antenna diversity schemes such as maximum ratio combining (MRC) are already in widespread use in communication systems. Since a large percentage of next generation mobile devices are expected to employ multiple antennas, it is essential to consider the effects of multiple antennas in the study of wireless systems.

A review of the literature reveals a rich set of articles related to optimization of wireless spectra as it pertains to power, bandwidth, and signal-to-noise ratio (SNR)/signal-to-interference ratio (SIR)/SINR. The references below are perhaps more closely related to the context of our current discussion. Andersin *et al.* [8], Bambos *et al.* [9], and Ulukus *et al.* [10] proposed various iterative methods to maximize the minimum SIR, to minimize total or individual power, or to maximize throughput under some kind of QoS constraint. Relying on geometric programming, a special case of convex optimization, Chiang *et al.* [11] solved a set of resource allocation problems for QoS provisioning in wireless ad-hoc networks. Kandukuri *et al.* [12] solved a similar problem aimed at minimization of the outage probability in cellular networks under Rayleigh fading without QoS constraints. Hayajneh *et al.* [13] proposed a game-theoretic power control algorithm for wireless channels. Shah *et al.* [14] and Ramanathan *et al.* [15] investigated the issue of power control in wireless networks with the considerations of network topology. Mahdavi-Doost *et al.* [16] considered interference in a communication system where each receiver only decodes its own data. They derived the zero-outage SINR region for an average power constraint and time-varying channel. Matskani *et al.* [17] considered a QoS constraint for the joint optimization of multiuser downlink beamforming and admission control. Their goal was to maximize the number of users satisfying the QoS constraint. They identified convex approximations of the solution since their optimal solution was non-deterministic polynomial-time (NP)-hard. Catrein *et al.* [18] studied the interference structure of multi-cell, multiuser code division multiple access (CDMA) systems and proposed admission control

Manuscript received July 21, 2010.

The authors would like to acknowledge Lynn Zheng for her involvement in an early research work related to this paper.

The authors are with the Center for Pervasive Communications and Computing (CPCC) at the University of California, Irvine; email: {hyousefi, hamidj}@uci.edu.

1229-2370/10/$10.00 © 2010 KICS

algorithms based on SINR. Chiang *et al.* [19] formulated power control problems as nonlinear optimization problems, showed that at high SIR such problems turn into geometric programming problems, and provided efficient global solutions for such problems. Zheng *et al.* [20] considered a single-input multiple-output multiuser system in which they minimized the transmit power of users under SINR constraints to find the optimal power control and receive beamforming vectors jointly.

Compared to the literature work cited above, this paper takes a different approach in trading off power-throughput under QoS constraints. To that end, the main contribution of our work is in the following areas. First, we model temporally correlated loss behavior of multiple antenna wireless fading channels by finite state Markov chains. Next, relying on our modeling results along with expressions of symbol error rates and dynamic achievable throughputs, we formulate and efficiently solve a pair of constrained resource allocation problems in a coherent framework for wireless ad-hoc networks.

The rest of this paper is organized as follows. In Section II, we assess the underlying system model. Our assessment includes an analysis of SINR, a treatment of the temporally correlated loss modeling, an evaluation of the expressions for symbol error rates, the use of Reed-Solomon channel coding technique, and the achievable dynamic throughput. In Section III, we formulate and solve a pair of resource allocation problems. While the first problem maximizes the overall system throughput subject to power and loss constraints, the second problem minimizes transmission power subject to throughput and loss constraints. Section IV provides validation results of our analysis. Finally, Section V concludes the paper.

II. SYSTEM MODEL ASSESSMENT

A. Analysis of Received Signal-to-Interference-Noise Ratio

Consider n wireless links, $\mathcal{L}_1, \cdots, \mathcal{L}_n$ on which transmission powers are $P_1, \cdots, P_n$, respectively. Each link may be connecting multiple antenna nodes. Suppose, the per symbol transmission power P_j is equally distributed among M_j transmit antennas of link j. The number of receive antennas for link j is assumed to be N_j. The nonnegative number $G_{ij}(t)$ represents the path gain in the absence of fading from the transmitter of link j to the receiver of link i at time t. $G_{ij}(t)$ captures such factors as path loss, shadowing, antenna gain, and so on. We denote $F_{ij}^{(m,n)}(t)$ as the fading factor between transmitting antenna m of link j and receiving antenna n of link i and assume that the paths between different pairs of transmit and receive antennas are independent. Then, the instantaneous SINR at time t for link i defined as the ratio of the desired received power at the receiver of link i over the interfering signals from all other links plus noise, specifies the quality of the received signal as defined below.

$$SINR_i(t) = \frac{G_{ii}(t)\frac{P_i(t)}{M_i}\sum_{m=1}^{M_i}\sum_{n=1}^{N_i}F_{ii}^{(m,n)}(t)}{\sum_{j\neq i}G_{ij}(t)\frac{P_j(t)}{M_j}\sum_{m=1}^{M_j}\sum_{n=1}^{N_i}F_{ij}^{(m,n)}(t)+N_i n_i(t)}. \quad (1)$$

We note that (1) considers the fact that the power of white Gaussian noise signal $n_i(t)$ on link i is multiplied by N_i receiving paths. Considering the magnitudes of the base and interference signals and the sources of the signals, we note that the fading factors between a transmitter and a receiver on different links are identically and independently distributed (i.i.d.). However, this assumption is not necessarily true when the transmitter and receiver belong to the same link. Generally speaking, the latter represents a temporally correlated channel in which the correlation between $F_{ij}(t)$ and $F_{ij}(t+\triangle t)$, where $\triangle t$ is a given time shift, cannot be ignored. In order to capture temporal correlation of the wireless channel, we make few realistic assumptions as follows. First, we assume that the fading factors in interfering signals F_{ij}'s where $i \neq j$, are i.i.d. We note that the latter assumption does not lead to a loss of generality as it may be relaxed relying on a similar discussion to the one furnished for the fading components F_{ii}. Second, F_{ij}'s have unit means so long as G_{ij}'s are appropriately scaled to reflect variations from this assumption. Third, the noise $n_i(t)$ has a mean of n_i. Fourth, when the wireless channel varies slowly with respect to symbol interval, $P_i(t)$ and $G_{ij}(t)$ can be viewed as constants and $F_{ij}(t)$ as a random variable within the symbol interval. Based on the above assumptions, we treat the average SINR for link i as a random variable in the form of

$$\begin{aligned} SINR_i &= \frac{E\left[G_{ii}(t)\frac{P_i(t)}{M_i}\sum_{m=1}^{M_i}\sum_{n=1}^{N_i}F_{ii}^{(m,n)}(t)\right]}{E\left[\sum_{j\neq i}G_{ij}(t)\frac{P_j(t)}{M_j}\sum_{m=1}^{M_j}\sum_{n=1}^{N_i}F_{ij}^{(m,n)}(t)+N_i n_i(t)\right]} \\ &= \frac{G_{ii}\frac{P_i}{M_i}\sum_{m=1}^{M_i}\sum_{n=1}^{N_i}F_{ii}^{(m,n)}}{\sum_{j\neq i}N_i G_{ij}P_j + N_i n_i} \end{aligned} \quad (2)$$

where $E[\cdot]$ represents the expectation operator. We also note that $F_{ii}^{(m,n)}$ in the second line of the equation above represents a random variable but the rest of the terms are constants. Given the probability density function (pdf) of the random variables $F_{ii}^{(m,n)}$ and under the assumption of spatial independence, the distribution of $SINR_i$ can be specified by deriving the convolution of the pdf of $F_{ii}^{(m,n)}$ [21]. Hence, it suffices to examine the distribution of $F_{ii}^{(m,n)}$ in order to obtain fading statistics of $SINR_i$. We start our discussion from the case of a link with single-transmit and single-receive antenna nodes, i.e., $F_{ii} = F_{ii}^{(1,1)}$ and $M_i = N_i = 1$. We refer to such case as a 1×1 link case. We rely on the Rice model with fading factor α and Rice factor κ to relate the output of a wireless noisy channel to its input. Albeit the fact that the Rice model describes a line-of-sight (LoS) wireless channel, setting $\kappa = 0$ reduces it to the Rayleigh model describing a rich scattering wireless channel.

For a network formed by a collection of LoS links, $r_{i,t} = |\alpha_{i,t}|$ representing the envelope of the fading signal of link i has a marginal Rician pdf [22] in the form of

$$p_R(r_{i,t}) = \frac{r_{i,t}(1+\kappa)}{\beta}\exp\left(-\kappa - \frac{(1+\kappa)r_{i,t}^2}{2\beta}\right)$$

$$\times I_0\left(2r_{i,t}\sqrt{\frac{\kappa(1+\kappa)}{2\beta}}\right),\quad r\geq 0 \tag{3}$$

where $\beta = E(r_{i,t}^2)/2$, κ is the Rice factor defined as the ratio of the dominant signal power component over the scattered power component, and I_0 is the zero-order modified Bessel function of the first kind given by $I_0(z) = \sum_{l=0}^{\infty}\frac{z^{2l}}{2^{2l}(l!)^2}$ with $z \geq 0$. In order to properly characterize the temporally correlated loss behavior of the channel, we also need the associated bivariate joint pdf given below [23].

$$\begin{aligned}
&p_{RR'}(r_{i,t}, r_{i,t'})\\
&= \frac{(1+\kappa)^2 r_{i,t}r_{i,t'}}{2\pi\beta^2(1-u^2)}\exp\left(\frac{-2\kappa}{1+u} - \frac{(1+\kappa)(r_{i,t}^2+r_{i,t'}^2)}{2(1-u^2)\beta}\right)\\
&\quad\times\int_0^{2\pi}\exp\left(\frac{u(1+\kappa)r_{i,t}r_{i,t'}\cos\theta}{(1-u^2)\beta}\right)\\
&\quad\times I_0\left(\sqrt{\frac{2\kappa(r_{i,t}^2+r_{i,t'}^2+2r_{i,t}r_{i,t'}\cos\theta)}{\beta(1+\kappa)^{-1}(1+u)^2}}\right)d(\theta),\\
&\quad r_{i,t}\geq 0,\ r_{i,t'}\geq 0.
\end{aligned} \tag{4}$$

In the equation above, t and t' are the time indices and $r_{i,t} = |\alpha_{i,t}|$ and $r_{i,t'} = |\alpha_{i,t'}|$ represent correlated Rician random variables. The random variables $\alpha_{i,t}$ and $\alpha_{i,t'}$ are then nonzero-mean correlated complex Gaussian with u representing the real correlation coefficient defined as

$$u = \frac{E((\alpha_{i,t'}^* - E(\alpha_{i,t'}^*))(\alpha_{i,t} - E(\alpha_{i,t})))}{\sqrt{E(|\alpha_{i,t'} - E(\alpha_{i,t'})|^2)}\sqrt{E(|\alpha_{i,t} - E(\alpha_{i,t})|^2)}}$$

where $\beta = E(r_{i,t}^2)/2 = E(r_{i,t'}^2)/2$ and $\theta = J_0(2\pi f_m\tau)$ with J_0 representing the zero-order Bessel function of the first kind defined as $J_0(z) = \sum_{l=0}^{\infty}\frac{(-1)^l z^{2l}}{2^{2l}(l!)^2}$ with $z \geq 0$. Finally, f_m and τ represent maximum frequency shift resulting from the Doppler effect and symbol duration, respectively. Considering the fact that F_{ii} is defined as $F_{ii} = r_i^2 = |\alpha_i|^2$, we are interested in the distribution of $|\alpha_i|^2$. Utilizing (3), (4), and the Jacobian technique [21], we conclude that F_{ii} has a marginal and a bivariate joint pdf as shown in (5) and (6), respectively.

$$\begin{aligned}
p(F_{ii}) &= 2\frac{F_{ii}(1+\kappa)}{\beta}\exp\left(-\kappa - \frac{(1+\kappa)F_{ii}}{\beta}\right)\\
&\quad\times I_0\left(\sqrt{\frac{4F_{ii}\kappa(1+\kappa)}{\beta}}\right),\quad F_{ii}\geq 0,
\end{aligned} \tag{5}$$

$$\begin{aligned}
&p(F_{ii,t}, F_{ii,t'})\\
&= \frac{(1+\kappa)^2\sqrt{F_{ii,t}F_{ii,t'}}}{2\pi\beta^2(1-u^2)}\\
&\quad\times\exp\left(-\frac{2\kappa}{1+u} - \frac{(1+\kappa)(F_{i,t}+F_{ii,t'})}{2(1-u^2)\beta}\right)\\
&\quad\times\int_0^{2\pi}\exp\left(\frac{u(1+\kappa)\sqrt{F_{i,t}F_{ii,t'}}\cos\theta}{(1-u^2)\beta}\right)\\
&\quad\times I_0\left(\sqrt{\frac{2\kappa(F_{ii,t}+F_{ii,t'}+2\sqrt{F_{ii,t}F_{ii,t'}}\cos\theta)}{\beta(1+\kappa)^{-1}(1+u)^2}}\right)d(\theta),\\
&\quad F_{ii,t}\geq 0,\ \ F_{ii,t'}\geq 0.
\end{aligned} \tag{6}$$

We also note that an alternative way of identifying the bivariate joint pdf of F_{ii} is proposed in [24]. Further, correlation coefficients of Rician envelope and power distributions are calculated in [25].

Next, we apply our formulation to the case of a 1×2 link. Given the joint pdf of $p(F_{ii,t}, F_{ii,t'})$ in the 1×1 case, we can specify the joint pdf of $p(F_{ii,t}^{(12)}, F_{ii,t'}^{(12)})$ in the 1×2 case as follows. We consider fading factors $F_{ii,t}^{(12)}$ and $F_{ii,t'}^{(12)}$ over link i at time instances t and t', respectively. Each fading factor consists of two components namely from the transmitter of the link to the first receiver of the link and from the transmitter of the link to the second receiver of the link. Hence, we have

$$\begin{aligned}
F_{ii,t}^{(12)} &= F_{ii,t}^{(1,1)} + F_{ii,t}^{(1,2)}\\
F_{ii,t'}^{(12)} &= F_{ii,t'}^{(1,1)} + F_{ii,t'}^{(1,2)}.
\end{aligned}$$

Under the assumption that there is no spatial correlation between any path pair, we note

$$\begin{aligned}
&p(F_{ii,t}^{(1,1)}, F_{ii,t}^{(1,2)}, F_{ii,t'}^{(1,1)}, F_{ii,t'}^{(1,2)})\\
&\quad= p(F_{ii,t}^{(1,1)}, F_{ii,t'}^{(1,1)})p(F_{ii,t}^{(1,2)}, F_{ii,t'}^{(1,2)}).
\end{aligned} \tag{7}$$

Each term of the right hand side of (7) can be calculated from (6). Next, we apply the Jacobian technique [21] to specify the joint pdf $p(F_{ii,t}^{(12)}, F_{ii,t'}^{(12)})$. We know that

$$\begin{aligned}
&p(F_{ii,t}^{(12)}, F_{ii,t'}^{(12)}, F_{ii,t}^{(1,1)}, F_{ii,t'}^{(1,1)})\\
&\quad= p(F_{ii,t}^{(1,1)} + F_{ii,t}^{(1,2)}, F_{ii,t'}^{(1,1)} + F_{ii,t'}^{(1,2)}, F_{ii,t}^{(1,1)}, F_{ii,t'}^{(1,1)})\\
&\quad= \frac{1}{|\mathcal{J}|}p(F_{ii,t}^{(12)} - F_{ii,t}^{(1,1)}, F_{ii,t'}^{(12)} - F_{ii,t'}^{(1,1)}, F_{ii,t}^{(1,1)}, F_{ii,t'}^{(1,1)})
\end{aligned} \tag{8}$$

where $|\mathcal{J}| = 1$ due to the fact that

$$\begin{aligned}
\mathcal{J} &= \begin{bmatrix}
\frac{\partial F_{ii,t}^{(12)}}{F_{ii,t}^{(1,1)}} & \frac{\partial F_{ii,t}^{(12)}}{F_{ii,t}^{(1,2)}} & \frac{\partial F_{ii,t}^{(12)}}{F_{ii,t'}^{(1,1)}} & \frac{\partial F_{ii,t}^{(12)}}{F_{ii,t'}^{(1,2)}}\\
\frac{\partial F_{ii,t'}^{(12)}}{F_{ii,t}^{(1,1)}} & \frac{\partial F_{ii,t'}^{(12)}}{F_{ii,t}^{(1,2)}} & \frac{\partial F_{ii,t'}^{(12)}}{F_{ii,t'}^{(1,1)}} & \frac{\partial F_{ii,t'}^{(12)}}{F_{ii,t'}^{(1,2)}}\\
\frac{\partial F_{ii,t}^{(1,1)}}{F_{ii,t}^{(1,1)}} & \frac{\partial F_{ii,t}^{(1,1)}}{F_{ii,t}^{(1,2)}} & \frac{\partial F_{ii,t}^{(1,1)}}{F_{ii,t'}^{(1,1)}} & \frac{\partial F_{ii,t}^{(1,1)}}{F_{ii,t'}^{(1,2)}}\\
\frac{\partial F_{ii,t'}^{(1,1)}}{F_{ii,t}^{(1,1)}} & \frac{\partial F_{ii,t'}^{(1,1)}}{F_{ii,t}^{(1,2)}} & \frac{\partial F_{ii,t'}^{(1,1)}}{F_{ii,t'}^{(1,1)}} & \frac{\partial F_{ii,t'}^{(1,1)}}{F_{ii,t'}^{(1,2)}}
\end{bmatrix}\\
&= \begin{bmatrix}
1 & 1 & 0 & 0\\
0 & 0 & 1 & 1\\
1 & 0 & 0 & 0\\
0 & 0 & 1 & 0
\end{bmatrix}.
\end{aligned}$$

Therefore, the joint pdf $p(F_{ii,t}^{(12)}, F_{ii,t'}^{(12)})$ can be calculated from the 2-way integral

$$\int_0^{\infty}\int_0^{\infty} p(F_{ii,t}^{(12)}, F_{ii,t'}^{(12)}, F_{ii,t}^{(1,1)}, F_{ii,t'}^{(1,1)})\ dF_{ii,t}^{(1,1)}dF_{ii,t'}^{(1,1)}. \tag{9}$$

Similarly, the cases of 2×1 and 2×2 links can be investigated. While in the former case the counter part of (9) will consist of a 2-way integral, in the latter case it will consist of a 4-way integral.

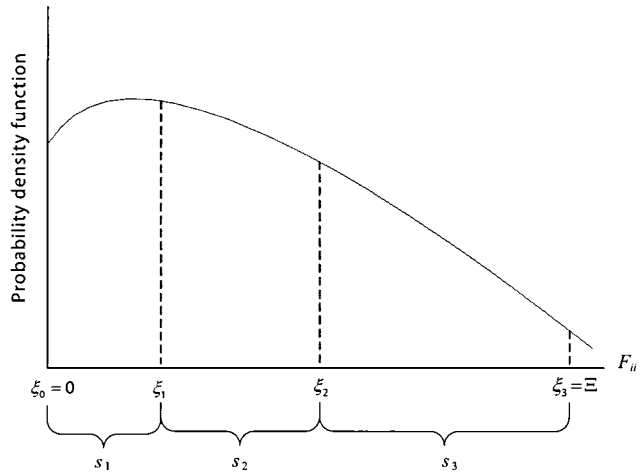

Fig. 1. An illustration of finite interval partitioning of an arbitrary pdf.

B. Markov Chain Channel Modeling

Having specified the probability density functions, we can now focus on capturing temporally correlated loss of the fading channel. We propose partitioning and modeling such analog channel with a digital Markov chain. A review of the literature reveals that there are numerous articles on partitioning the received SNR, SIR, or SINR. References [4] and [5] are of special interest to us among those articles. In our work, we apply the fundamental idea of partitioning to the pdf of F_{ii} in order to model the fading channel with a finite-state Markov chain. We note that in its general form, F_{ii} may represent the pdf of an $M_i \times N_i$ link. While the discussion below is applied to a 1×1 case, its extension to other antenna configurations is straight forward. As illustrated by Fig. 1, suppose that the pdf of F_{ii} is partitioned into $S+1$ finite threshold values $\{\xi_0, \cdots, \xi_S\}$ starting at zero and ending at Ξ. Ξ is a large real number satisfying

$$\int_0^{\Xi} p(F_{ii}) dF_{ii} = 1 - \delta \tag{10}$$

where δ, e.g. 10^{-5}, indicates the probability of not representing a value of the pdf of F_{ii} by any state. Given the threshold values, $\{\xi_0, \cdots, \xi_S\}$, one can find $F_{ii,s}$, the representative value of the conditional pdf of F_{ii} in state s, as

$$F_{ii,s} = \int_{\xi_{s-1}}^{\xi_s} F_{ii}\, p(F_{ii})\, dF_{ii}, \quad s = 1, \cdots, S. \tag{11}$$

We discuss how to calculate the threshold values at the end of this section. Using (11), the corresponding representative values of $SINR_i$'s in the 1×1 case are given by

$$SINR_{i,s} = \frac{G_{ii} P_i F_{ii,s}}{\sum_{j \neq i} G_{ij} P_j + N_i n_i}, \quad s = 1, \cdots, S. \tag{12}$$

The temporal dynamics of the Markov chain are determined by a matrix of one-step-transition probabilities $\Pi = [\pi_{sr}]_{S \times S}$. Since we are working with slow-fading channels, it is reasonable to consider only transitions between neighboring states or staying in the same state [4]. According to Bayes theorem, the probability of currently being in state r given having previously been in state s can be computed as[1]

$$\tilde{\pi}_{sr} = \frac{\int_{\xi_{r-1}}^{\xi_r} \int_{\xi_{s-1}}^{\xi_s} p(F_{ii,t}, F_{ii,t'})\ dF_{ii,t} dF_{ii,t'}}{\int_{\xi_{s-1}}^{\xi_s} p(F_{ii})\ dF_{ii}} \tag{13}$$

where $r \in \{s, s \pm 1\}$ and for $1 \leq r, s \leq S$.

Due to the finite value of the error introduced by the model and the transitioning assumption, we must modify the transition matrix such that each row adds up to one. This can be done by uniformly scaling each row by its sum as $\pi_{sr} = \tilde{\pi}_{sr} / \sum_{s=1}^{S} \tilde{\pi}_{sr}$.

To complete the discussion of this section, we need to identify the partitioning thresholds $\{\xi_0, \cdots, \xi_S\}$. In what follows, we provide two alternatives of specifying the thresholds. In the first alternative, the partitioning thresholds can be set from the observed average natural burst lengths of a wireless channel using the proposal of [26]. In [26], the authors consider a 2-state Markov chain in which $s = 1$ and $s = 2$ represent a good and a bad channel state quality, respectively. The observed average burst length of receiving BL_1 symbols correctly is mapped to the transition probability $\tilde{\pi}_{12}$ as $BL_1 = 1/\tilde{\pi}_{12}$. Similarly, the observed average burst length of losing BL_2 symbols is mapped to the transition probability $\tilde{\pi}_{21}$ as $BL_2 = 1/\tilde{\pi}_{21}$. Once the transitioning probabilities are identified, the set of threshold values are numerically set using (13) such that they match the transition probabilities. We also note that the measurement of burst lengths can be extended to a larger number of states.

In the second alternative to which we refer as the γ-scaled partitioning approach, the set of thresholds $\{\xi_1, \cdots, \xi_S\}$ are set such that

$$\begin{aligned} &\int_{\xi_{s-1}}^{\xi_s} p(F_{ii})\ dF_{ii} = \gamma_i \frac{1-\delta}{S}, \\ &s = 1, \cdots, S, \quad \xi_0 = 0, \quad \xi_S = \Xi, \\ &\sum_{i=1}^{S} \gamma_i = S. \end{aligned} \tag{14}$$

Comparing the two alternatives, we mention that the first alternative is a more realistic representation of the wireless channel, compare to the second alternative, at a higher complexity cost.

At the end of this subsection, we note that the above discussion is valid for fading scenarios in which channel coefficients change from a symbol to the next symbol. However, many coding scenarios work with a quasi-static fading assumption in which channel coefficients change from a block to the next block but remain the same in a block duration. This is practically justified because channel estimation is only available on a per block basis due to the use of one set of pilot symbols per block. In a quasi-static fading case, a similar approach can be used to identify the parameters of a Markov chain associated with the blocks

[1] Note that depending on the antenna configurations, calculating the numerator of (13) may result in a higher dimension integral. For example, it results in calculating 2-way, 4-way, 4-way, and 8-way integrals in the cases of 1×1, 1×2, 2×1, and 2×2 antenna configurations, respectively.

as oppose to symbols. We refer the interested reader to [27] where a similar discussion is carried out to go from a Markov chain at the bit level to a Markov chain at the symbol level.

C. Calculation of Symbol Error Rate for Multiple Antenna Systems

In this section, we calculate the symbol error rate of a multiple-input multiple-output (MIMO) link under the assumption of facing a LoS fading Rician channel and utilizing L-phase shift keying (PSK) modulation. We also note that our approach can be applied to other modulation schemes such as quadrature amplitude modulation (QAM).

First, we introduce the symbol error rate of a Rician fading link associated with single-transmit and N-receive antenna nodes using MRC. Starting from (9.15) of [28], the symbol error rate of a single-transmit N-receive antenna system using MRC can be calculated as

$$SER = \frac{1}{\pi}\int_0^{(L-1)\pi/L}\left[\frac{(1+\kappa)\sin^2\phi}{\overline{SINR}\sin^2(\frac{\pi}{L})+(1+\kappa)\sin^2\phi)} \times \exp\left(-\frac{\kappa\overline{SINR}\sin^2\left(\frac{\pi}{L}\right)}{\overline{SINR}\sin^2(\frac{\pi}{L})+(1+\kappa\sin^2\phi)}\right)\right]^N d\phi. \quad (15)$$

While there is no closed-form solution to the integral above, its value can be numerically evaluated. We note that the integral is reduced to the case of Rayleigh fading for non-line-of-sight (NLoS) fading environments with $\kappa = 0$ for which the closed-form solution below is available.

$$SER = \frac{L-1}{L} - \frac{1}{\pi}\sqrt{\frac{\vartheta}{1+\vartheta}}\{(\frac{\pi}{2}+\tan^{-1}\xi) \times \sum_{j=0}^{N-1}\binom{2j}{j}\frac{1}{[4(1+\vartheta)]^j} + \sin(\tan^{-1}\xi) \times \sum_{j=1}^{N-1}\sum_{i=1}^{j}\frac{\sigma_{ij}}{(1+\vartheta)^j}[\cos(\tan^{-1}\xi)]^{2(j-i)+1}\} \quad (16)$$

where $\vartheta = SINR\sin^2(\frac{\pi}{L})$, $\xi = \sqrt{\frac{\vartheta}{1+\vartheta}}\cot\frac{\pi}{L}$, and $\sigma_{ij} = \frac{\binom{2j}{j}}{\binom{2(j-i)}{j-i}4^i[2(j-i)+1]}$. From (15) or (17), one can calculate the symbol error rate of a link associated with single-transmit single-receive antenna nodes as well as a link associated with single-transmit double-receive antenna nodes by setting N to 1 and 2, respectively. As discussed in Section 4.9 of [29], the symbol error rate of orthogonal STBCs can be calculated from (15) by proper mapping of the values of $SINR$. For example, the symbol error rate of a 2×1 Rician link can be calculated by setting N to 2 in (15) and using appropriate $SINR$ from the counter part of (12) in the case of 2×1 antenna configuration.

D. Compensation of Temporally Correlated Loss

In order to compensate for the loss effects of the wireless channel, we propose the use of reed-solomon (RS) channel coders. An RS channel coder $RS(b,k)$ converts k symbols into a b-symbol block[2] by appending $(b-k)$ parity symbols. Such a channel coder is able to correct as many as $t_C = \lfloor\frac{b-k}{2}\rfloor$ symbol errors in a block. In the calculation of the block-loss probability, we consider using a 2-state Markov chain model depicted in Fig. 2, and a 3-state Markov chain model shown in Fig. 3. Intuitively, the 3-state model is more accurate than its 2-state counterpart, at the cost of higher computational complexity. Equations (5), (6), (11), (13), and (14) have given the details of deriving transition probabilities $\tilde{\pi}_{sr}$'s from marginal and joint probability density functions.

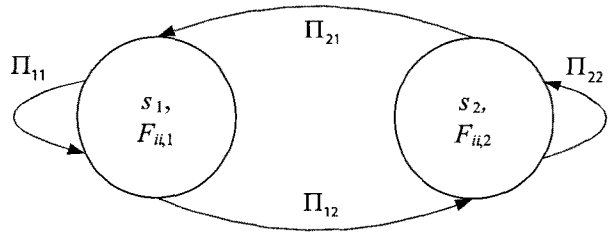

Fig. 2. An illustration of the 2-state Markov chain model.

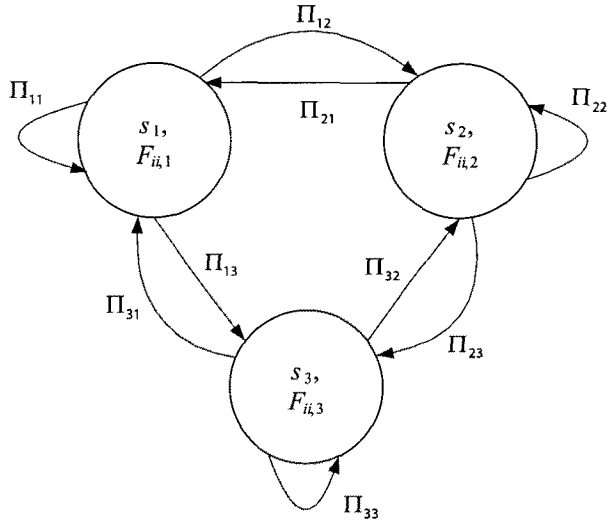

Fig. 3. An illustration of the 3-state Markov chain model.

Let $\varphi(b,k,s)$ denote the probability of receiving exactly k symbols from b symbols and winding up in state s. The probability of receiving exactly k symbols from a b-symbol block is given by

$$\varphi(b,k) = \sum_{s=1}^{S}\varphi(b,k,s). \quad (17)$$

If a user receives at least $b - t_C$ symbols correctly from b transmitted symbols, the whole block is recoverable. Hence, the block-loss probability is expressed as

$$\Psi = 1 - \sum_{k=b-t_C}^{b}\varphi(b,k). \quad (18)$$

Next, we apply the block loss probability results to the 2-state and 3-state Markov chains. First, we consider using a 2-state

[2]It is important to differentiate between an STBC coding block with an RS channel coding block mentioned in this section.

Markov chain model. We assume $\varphi(b,k,1)$ and $\varphi(b,k,2)$ indicate the probabilities of receiving exactly k symbols from b symbols and winding up in state 1 and state 2, respectively. Thus,

$$\varphi(b,k) = \varphi(b,k,1) + \varphi(b,k,2). \tag{19}$$

In accordance with the underlying Markov chain model, $\varphi(b,k,1)$ and $\varphi(b,k,2)$ can be computed recursively. The expressions are given below.

$$\begin{aligned}\varphi(b,k,1) &= SER_1[\pi_{11}\varphi(b-1,k,1) + \pi_{21}\varphi(b-1,k,2)] \\ &\quad + (1-SER_1)[\pi_{11}\varphi(b-1,k-1,1) \\ &\quad + \pi_{21}\varphi(b-1,k-1,2)]\end{aligned} \tag{20}$$

and

$$\begin{aligned}\varphi(b,k,2) &= SER_2[\pi_{12}\varphi(b-1,k,1) + \pi_{22}\varphi(b-1,k,2)] \\ &\quad + (1-SER_2)[\pi_{12}\varphi(b-1,k-1,1) \\ &\quad + \pi_{22}\varphi(b-1,k-1,2)]\end{aligned} \tag{21}$$

for $b \geq k > 0$, SER_s denoting the symbol error rate in state s, and the initial conditions

$$\begin{aligned}\varphi(0,0,1) &= \varphi(0,0,2) = \frac{1}{2}, \\ \varphi(1,0,1) &= SER_1[\pi_{11}\varphi(0,0,1) + \pi_{21}\varphi(0,0,2)], \\ \varphi(1,0,2) &= SER_2[\pi_{12}\varphi(0,0,1) + \pi_{22}\varphi(0,0,2)], \\ \varphi(1,1,1) &= (1-SER_1)[\pi_{11}\varphi(0,0,1) + \pi_{21}\varphi(0,0,2)], \\ \varphi(1,1,2) &= (1-SER_2)[\pi_{12}\varphi(0,0,1) + \pi_{22}\varphi(0,0,2)].\end{aligned} \tag{22}$$

Similarly, if a 3-state Markov chain model is used, we have

$$\varphi(b,k) = \varphi(b,k,1) + \varphi(b,k,2) + \varphi(b,k,3) \tag{23}$$

where

$$\begin{aligned}\varphi(b,k,1) &= SER_1[\pi_{11}\varphi(b-1,k,1) + \pi_{21}\varphi(b-1,k,2)] \\ &\quad + (1-SER_1)[\pi_{11}\varphi(b-1,k-1,1) \\ &\quad + \pi_{21}\varphi(b-1,k-1,2)],\end{aligned} \tag{24}$$

$$\begin{aligned}\varphi(b,k,2) &= SER_2[\pi_{12}\varphi(b-1,k,1) + \pi_{22}\varphi(b-1,k,2) \\ &\quad + \pi_{32}\varphi(b-1,k,3)] \\ &\quad + (1-SER_2)[\pi_{12}\varphi(b-1,k-1,1) \\ &\quad + \pi_{22}\varphi(b-1,k-1,2) \\ &\quad + \pi_{32}\varphi(b-1,k,3)],\end{aligned} \tag{25}$$

and

$$\begin{aligned}\varphi(b,k,3) &= SER_3[\pi_{23}\varphi(b-1,k,2) + \pi_{33}\varphi(b-1,k,3)] \\ &\quad + (1-SER_3)[\pi_{23}\varphi(b-1,k-1,2) \\ &\quad + \pi_{33}\varphi(b-1,k-1,3)]\end{aligned} \tag{26}$$

for $b \geq k > 0$ and the initial conditions

$$\begin{aligned}\varphi(0,0,1) &= \varphi(0,0,2) = \varphi(0,0,3) = \frac{1}{3}, \\ \varphi(1,0,1) &= SER_1[\pi_{11}\varphi(0,0,1) + \pi_{21}\varphi(0,0,2)], \\ \varphi(1,0,2) &= SER_2[\pi_{12}\varphi(0,0,1) + \pi_{22}\varphi(0,0,2) \\ &\quad + p_{32}P(0,0,3)], \\ \varphi(1,0,3) &= SER_3[\pi_{23}\varphi(0,0,2) + \pi_{33}\varphi(0,0,3)], \\ \varphi(1,1,1) &= (1-SER_1)[\pi_{11}\varphi(0,0,1) + \pi_{21}\varphi(0,0,2)], \\ \varphi(1,1,2) &= (1-SER_2)[\pi_{12}\varphi(0,0,1) + \pi_{22}\varphi(0,0,2) \\ &\quad + \pi_{32}\varphi(0,0,3)], \\ \varphi(1,1,3) &= (1-SER_3)[\pi_{23}\varphi(0,0,2) + \pi_{33}\varphi(0,0,3)].\end{aligned} \tag{27}$$

E. Achievable Adaptive Throughput

In this section, we describe the expression for the achievable adaptive throughput. In the adaptive throughput expression, the value of per link throughput R_i is expressed as

$$R_i = \sum_{s=1}^{S} \omega_s R_{i,s} = \epsilon \frac{r_i}{T} \sum_{s=1}^{S} \omega_s \log_2 L_{i,s} \tag{28}$$

where $1/T$ is the baseband bandwidth, ϵ is the scaling factor of the transmission energy to the bandwidth, $r_i = k_i/b$ is the channel coding rate in $RS(b,k_i)$, and ω_s the set of steady state probabilities of being in state s can be calculated from the transition probabilities of a given Markov chain. For example, for $S = 2$, we have

$$\begin{aligned}\omega_1 &= \frac{\pi_{21}}{\pi_{12}+\pi_{21}}, \\ \omega_2 &= \frac{\pi_{12}}{\pi_{12}+\pi_{21}}.\end{aligned}$$

We note that the use of (28) can translate to the use of adaptive modulation if the values of $L_{i,s}$ are to be chosen dynamically, adaptive channel coding rates if the values of r_i are to be chosen dynamically, or both adaptive modulation and adaptive channel coding rates.

At the end of this section, a discussion of channel state information (CSI) is in order. We assume that the CSI is unknown at a transmitting node. Therefore, the set of per link per state parameters $L_{i,s}$ are reduced to a set of per link parameters L_i. We note that for the case of a known CSI, more effective transmission techniques such as beamforming can be employed. The discussion of such techniques is outside the scope of this paper.

III. RESOURCE ALLOCATION PROBLEMS

In this section, we formulate our problem and provide a solution to it. From the perspective of a system, we seek to maximize the overall system throughput under the constraints related to per link block-loss probabilities, minimum link throughput, and powers. In addition, we also seek to minimize the power of transmission under the constraints related to throughputs, minimum link throughputs, and per link block-loss probabilities. For clarity of discussion, we assume the use of adaptive modulation and fixed channel coding. We note that the discussion of problem formulations and solutions below can also be applied to a

case in which fixed modulation and adaptive channel coding are used by replacing all of the variables L_i with r_i. Further, they can be easily extended to a case in which adaptive modulation and adaptive channel coding are jointly used. In such a case, all of the expressions including variables L_i are extended to additionally include variables r_i.

The throughput maximization problem appears in the following form.

$$\max_{P_i,L_i} R_{\text{total}} = \sum_{i=1}^{n} R_i \tag{29}$$

$$\begin{aligned} \text{Subject to:} \quad & \Psi_i \le \Psi_{i,ub}, \quad \forall i \in \{1,\cdots,n\}, \\ & R_i \ge R_{i,lb}, \quad \forall i \in \{1,\cdots,n\}, \\ & P_i \le P_{i,ub}, \quad \forall i \in \{1,\cdots,n\}. \end{aligned} \tag{30}$$

We note that in the formulation above, P_i's and L_i's are the decision variables. Further, we note that the SER parameters of the Markov chain discussion of Section II-D appear in the form of a set of per link parameters. It is also important to note that the constrained maximization problem formulated above is converted to a constrained power minimization problem by defining a second objective function in the form of $P_{\text{total}} = \sum_{i=1}^{n} P_i$ and applying a similar set of constraints. The power minimization problem is then expressed as

$$\min_{R_i,L_i} P_{\text{total}} = \sum_{i=1}^{n} P_i \tag{31}$$

$$\begin{aligned} \text{Subject to:} \quad & \Psi_i \le \Psi_{i,ub}, \quad \forall i \in \{1,\cdots,n\}, \\ & \sum_{i=1}^{n} R_i \ge R_{lb}, \\ & P_i \le P_{i,ub}, \quad \forall i \in \{1,\cdots,n\}. \end{aligned} \tag{32}$$

Equations (2), (15), (17), and (28) show that the throughputs R_i are related with per link constellation sizes L_i. Therefore, the objective function (29) is to be optimized over all feasible powers and constellation sizes. The first set of constraints in (30) and (32) represent the maximum allowable block-loss probability on each link. The second set of constraints in (30) and (32) are enforced to assure each link or the collection of links receive a minimum guaranteed throughput. Same as the objective function, this set is related to L_i's. We note that the latter constraint set may be relaxed if there is no minimum guaranteed throughput. The last set of constraints in (30) and (32) indicate regulatory or system limitations on transmission powers. As shown by (15) (or (17)) through (27), Ψ_i's are essentially functions of per link SER_i's, hence of P_i's as well as L_i's.

Next, we provide a discussion of solving the optimization problem formulated by (29) along with the constraint sets (30). We note that the solution to the optimization problem formulated by (31) along with the constraint sets (32) is derived similarly. Relying on the Lagrangian theory, we convert the problem in its standard form to an optimization problem without constraints. We define the Lagrangian function of the original problem as

$$\begin{aligned} \Lambda = & -\sum_{i=1}^{n} R_i + \sum_{i=1}^{n} \lambda_i(\Psi_i - \Psi_{i,ub}) \\ & + \sum_{s=1}^{S}\sum_{i=1}^{n} \rho_i(-R_i + R_{i,lb}) \\ & + \sum_{i=1}^{n} \nu_i(P_i - P_{i,ub}) \end{aligned} \tag{33}$$

where the parameters λ_i, ρ_i, and ν_i are the Lagrange multipliers in the Lagrangian Equation (33). The unconstrained minimization problem is defined as

$$\begin{aligned} \min_{P_i,L_i} \Lambda = & \min_{L_i,P_i}\{-\sum_{i=1}^{n} R_i \\ & + \sum_{i=1}^{n} \lambda_i(\Psi_i - \Psi_{i,ub}) \\ & + \sum_{s=1}^{S}\sum_{i=1}^{n} \rho_i(-R_i + R_{i,lb}) \\ & + \sum_{i=1}^{n} \nu_i(P_i - P_{i,ub})\}. \end{aligned} \tag{34}$$

Conditions of optimality: Constraint qualifications

We now investigate the existence of necessary and sufficient optimality conditions also known as constraint qualifications. For our unconstrained minimization problem of (34), the constraint qualifications are expressed in terms of Lagrange multiplier theory [30]. They revolve around conditions under which Lagrange multiplier vectors satisfying the following conditions are guaranteed to exist for a local optimum $\Omega^* = \{P_i^*, L_i^*\}$ that satisfies $\nabla\Lambda(\Omega^*) = 0$ where $\nabla\Lambda = [\frac{\partial\Lambda}{\partial P_i}, \frac{\partial\Lambda}{\partial L_i}]$.

Although the first set of constraints in (30) cannot be expressed in closed-forms, we are able to solve the problem by deploying sequential quadratic programming (SQP) and line search techniques. In SQP, necessary conditions for optimality are represented by the karush-kuhn-tucker (KKT) conditions described as the collection of $\nabla\Lambda(\Omega^*) = 0$ and the following relationships.

$$\begin{aligned} & \lambda_i{}^*(\Psi_i{}^* - \Psi_{i,ub}) = 0, \quad \rho_i{}^*(-R_i{}^* + R_{i,lb}) = 0, \quad \forall i, \\ & \nu_i{}^*(P_i{}^* - P_{i,ub}) = 0, \quad \lambda_i{}^*, \rho_i{}^*, \nu_i{}^* \ge 0, \quad \forall i \end{aligned} \tag{35}$$

where $\lambda_i{}^*$, $\rho_i{}^*$, and $\nu_i{}^*$ are Lagrange multipliers at the local optimum. Positive multipliers indicate active constraints. A variant of the quasi-Newton method can then be used to iteratively find the solution to the optimization problem [31]. This is equivalent to solving a quadratic estimation of the problem in every iteration.

At the end of this section, we present an analysis of the computational complexity for the approach described above. The time complexity of solving $\nabla\Lambda(\Omega^*) = 0$ is $\mathcal{O}(I\,\zeta\,\log\zeta)$ where I indicates the number of iterations and ζ indicates the degree of the quadratic estimation. For moderate values of I, the complexity results are quite good compared to other recursive optimization approaches such as dynamic programming introducing

a time complexity in the order of $\mathcal{O}(\zeta^2)$.

Finally, we note that the formulations of our problem can be applied either to an overall topology or on a per node basis with a sub-topology of links attached to the node. While the former case represents a centralized problem, the latter case represents a decentralized problem. In the latter case, the sum of the throughputs or the powers of the links using a given node as their transmitting node is optimized subject to a set of constraints. Similar to the objective functions, the set of constraints are only applied to the links of a given node.

IV. NUMERICAL ANALYSIS

In this section, we present our simulation results. Before proceeding with the explanation of our numerical results, we note that we are solving throughput and power optimization problems in wireless ad-hoc networks accommodating nodes with both single and double antennas. In the case of a double antenna transmission, we assume that two signals are transmitted simultaneously from the two transmit antennas at each time slot using orthogonal STBCs. In the case of double antenna receive, we assume that MRC is used. In addition, we also assume that the slow fading wireless channel characterized by a Rician or Rayleigh distribution is quasi-static and flat implying that the fading factors are constant over a coding block but vary from one block to another.

A. Throughput Maximization

In this section, we report sample results of our simulations utilizing the throughput maximization scheme of the previous section. The results of the centralized optimization problem are provided for Rician LoS fading environments. We consider two cases in which a node is either equipped with one or two antennas. In the case of a double-transmit antenna node, we assume that two signals are transmitted simultaneously from the two antennas at each time slot using an orthogonal STBC. In addition, we assume that the fading wireless channel is characterized by a Rician distribution with parameters $\kappa = 0.125$ and $\beta = 4.5$. We, further, assume the CSI is unknown at transmitting nodes but known at receiving nodes. While outside the scope of this paper, we note that the use of beamforming techniques may result in a significant performance enhancement in case the CSI is known at the transmitting nodes.

We apply our results to an ad-hoc network topology illustrated in Fig. 4. The network parameters are chosen such that the network simulates the communication of four nodes leveraging LoS communication paths. The network consists of nodes A, B, C, and D, along with 4 links $\mathcal{L}_1$ through $\mathcal{L}_4$. Each node is able to transmit and/or a receive on multiple links given it cannot transmit and receive at the same time. In the case of simultaneously transmitting on multiple links, the transmission power is split on the outgoing links equally.

Originally, nodes A and D are separated by a distance of 320 km, and so are B and C. We allow node A to move across the horizontal axis both toward and away from node D. The position of node A from a reference point is indicated by x. We select the reference point to be the middle of the diagonal line connecting nodes B and C. Hence, the original position of node A is indicated by $x = 160$ km. We consider four different scenarios:

(1) all of the nodes are single-antenna nodes,
(2) node A has double antennas utilizing orthogonal STBCs and the rest of the nodes have a single antenna,
(3) node D has double antennas utilizing MRC and the rest of the nodes have a single antenna, and
(4) node A has double antennas utilizing orthogonal STBCs, node D has double antennas utilizing MRC, and the rest of the nodes have a single antenna.

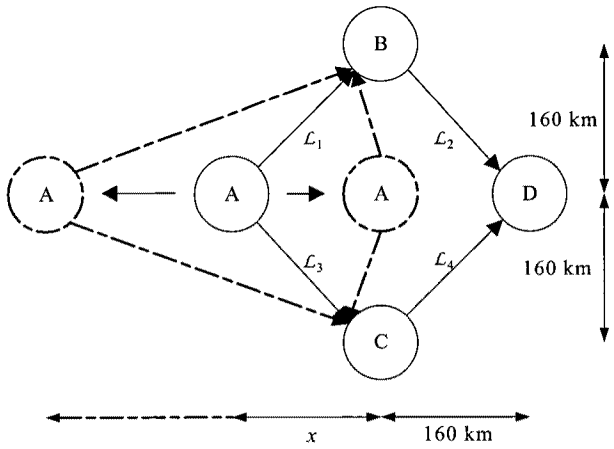

Fig. 4. A sample network topology used in the throughput maximization simulation task.

In our simulations, each link has a minimum and a maximum transmission power of 0.1 W and 4 W, respectively. Further, the average power of noise is assumed to be 10 μW. We note that the average power of noise can potentially capture the effects of signal interference from other active nodes in the vicinity of a given node and not shown in the topology. However, we assume the minimal existence of such effects in our simulations. All nodes are using adaptive RS codes with a block size of 31 and fixed binary-PSK (BPSK) modulation. The baseband broadband bandwidth for each link is $\frac{1}{T} = 2$ GHz with $\epsilon = 2.5 \times 10^{-4}$ and the minimum guaranteed throughput for each link is 128 Kbps. A maximum allowable block-loss probability of 10^{-6} is set on each link. With the exception of G_{12} and G_{34}, the gains for each link are computed as $G_{ii} = \frac{2.56}{d_{ii}^2}$ and $G_{ij} = \frac{\eta}{d_{ij}^2}$ for $i \neq j$ where d_{ij} represents propagation path length from the transmitter of link j to the receiver of link i. The factor η is set to 0.0128 in our simulations. The gains for G_{12} and G_{34} are set to 0 since we assume a node cannot transmit and receive at the same time. This gives the following gain matrix G in terms of x

$$\begin{bmatrix} \frac{2.56}{x^2+160^2} & 0 & \frac{\eta}{x^2+160^2} & \frac{\eta}{320^2} \\ \frac{\eta}{(x+160)^2} & \frac{2.56}{51200} & \frac{\eta}{(x+160)^2} & \frac{\eta}{320^2} \\ \frac{\eta}{x^2+160^2} & \frac{\eta}{320^2} & \frac{2.56}{x^2+160^2} & 0 \\ \frac{\eta}{(x+160)^2} & \frac{\eta}{51200} & \frac{\eta}{(x+160)^2} & \frac{2.56}{51200} \end{bmatrix}. \quad (36)$$

Working with the 2-state Markov chain fading model in the case of a 1×1 link with average channel symbol burst lengths of 1600 and 16, we calculate the values of $\pi_{21} = 0.125$ and $\pi_{12} = 0.00127$ for a coding block consisting of two symbols. The latter translates to a threshold vector of [0 1 40]. In

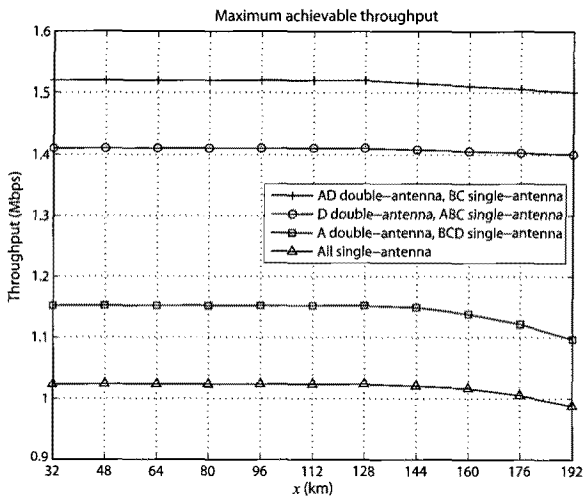

Fig. 5. Optimal curves of total achievable throughput versus x.

Table 1. The range of the optimal values of $RS(b, k_i^*)$ identifying $r_i^* = k_i^*/b$ over different links for different scenarios.

Scenario	$\mathcal{L}_1, \mathcal{L}_3$	$\mathcal{L}_2, \mathcal{L}_4$
(1)	[15/31, 17/31]	[15/31, 17/31]
(2)	[23/31, 25/31]	[19/31, 21/31]
(3)	[23/31, 25/31]	[19/31, 21/31]
(4)	[20/31, 24/31]	[22/31, 26/31]

order to comply with the notion of fairness, we keep the partitioning thresholds the same in the case of other antenna configurations. Fig. 5 shows the curves of optimal total throughput versus x the position of node A for the different antenna scenarios described above. The curves show that the throughputs are maintained relatively flat in the range of $x \in [32, 144]$ km. As x increases beyond 144 km, the throughput is decreased due to the loss of signal strength. The striking observation when comparing the results of individual figures is the fact that the optimal throughput of scenario (1) is consistently lower than that of the rest. For a given transmission power, we expect to see a higher throughput when using more antennas. Comparing the throughput of scenario (2) with that of scenario (3), we observe that the former introduces a lower optimal throughput due to the fact that for a fixed $SINR$ the power efficiency of the former scheme suffers a 3 dB loss compared to that of the latter scheme for the same transmission power. Finally, we note that the throughput of scenario (4) is the best among the four scenarios.

Table 1 illustrates the range of optimal values of $RS(b, k_i^*)$ identifying $r_i^* = \frac{k_i^*}{b}$ over different links for the antenna scenarios described above.

We end this section by commenting on our complexity results. We have observed that an average of ten and no more than twelve iterations are required for convergence. Further, we have observed that utilizing a 3-state Markov chain increases maximum achievable throughput compared to the case of a 2-state Markov chain, at the cost of a higher overhead of calculation.

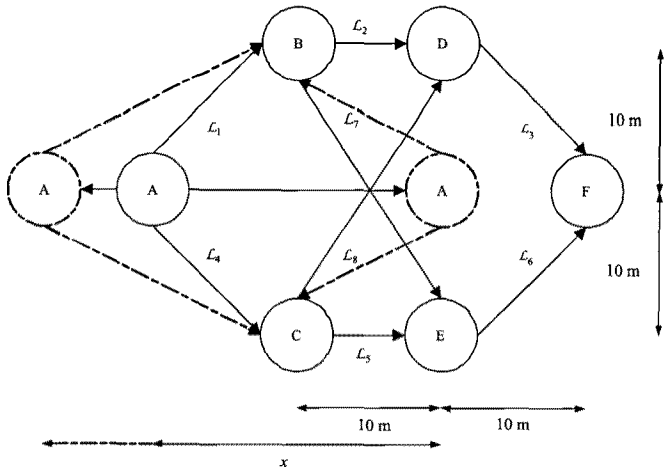

Fig. 6. An illustration of the network topology used in the power optimization simulation task.

B. Power Minimization

In this section, we report sample results of simulations utilizing the power minimization scheme of the previous sections. The results are provided for Rayleigh rich scattering fading environments over a sample topology by setting $\kappa = 0$ in (15). We again consider two cases in which a node is either equipped with one or two antennas. In the case of a double-transmit antenna node, we assume that two signals are transmitted simultaneously from the two antennas at each time slot using STBCs. In addition, we assume the CSI is unknown at transmitting nodes but known at receiving nodes.

We apply our results to an ad-hoc network topology as illustrated in Fig. 6. The network consists of nodes A, B, C, D, E, and F, along with 8 links $\mathcal{L}_1$ through $\mathcal{L}_8$. Each link can act both as a transmitter and a receiver. We also assume that a node can simultaneously transmit on multiple links by splitting its power on outgoing links. Originally, the topology is symmetric with horizontal and vertical line segments of 10 m each. By geometry the distance of single hops $\mathcal{L}_3$ and $\mathcal{L}_6$ is $10\sqrt{2}$ m. Similarly, the distance of the single hops $\mathcal{L}_7$ and $\mathcal{L}_8$ is $10\sqrt{5}$ m. In our simulations, we allow node A to move across the horizontal axis x both toward and away from node F. Again, we indicate the position of node A from a reference point by x. We select the reference point to be the middle of vertical line connecting nodes D and E. Hence, the original position of node A is indicated by $x = 20$ m. We consider four different scenarios:

(1) nodes B, C, and F are single antenna nodes while the rest are double antenna nodes,
(2) nodes B and C are single antenna nodes while the other nodes are double antenna nodes,
(3) node A has a single antenna and the rest of the nodes have double antennas, and
(4) all nodes have double antennas.

In our simulations, the lower and upper regulatory power bounds are set at 0.001 W and 1 W, respectively. The average power of noise is assumed to be 10 μW. All nodes are using fixed $RS(31, 15)$ coders and adaptive L-PSK modulation representing a symbol with $\log_2 L_i$ bits per link. The baseband wideband bandwidth for each link is $1/T = 100$ KHz with $\epsilon = 2.0666$

and the target aggregate throughput is 2 Mbps. We set a maximum allowable block-loss probability of 0.005. In this rich scattering environment, the gains for each link are computed as $G_{ii} = 1/d_{ii}^4$ and $G_{ij} = \eta/d_{ij}^4$ for $i \neq j$, where d_{ij} represents propagation path length from the transmitter of link j to the receiver of link i. The factor η is set as $\eta = 0.005$ in our simulations.

Just like the previous subsection, the channel is assumed to introduce average symbol burst lengths of 1600 and 16 in the case of partitioning a single-transmit single-receive antenna configuration. The latter numbers correspond to the values of $\pi_{21} = 0.125$ and $\pi_{12} = 0.00127$ for a coding block consisting of two symbols and a threshold vector of [0 1 10]. In order to comply with the notion of fairness, we keep the partitioning thresholds the same in the case of other antenna configurations. In this case, the gain matrix G is an 8×8 matrix. The gains for G_{12}, G_{17}, G_{23}, G_{45}, G_{48}, G_{56}, G_{76}, and G_{83} are set to 0 since a node does not transmit to itself. The gain matrix is represented in the form of

$$G = [G_L|G_R]. \tag{37}$$

The matrix G_L appears in the following form

$$\begin{bmatrix}
\frac{1}{((x-10)^2+100)^2} & 0 & \frac{\eta}{100^2} & \frac{\eta}{((x-10)^2+100)^2} \\
\frac{\eta}{(x^2+100)^2} & \frac{1}{100^2} & 0 & \frac{\eta}{(x^2+100)^2} \\
\frac{\eta}{(x+10)^4} & \frac{\eta}{500^2} & \frac{1}{200^2} & \frac{\eta}{(x+10)^4} \\
\frac{\eta}{((x-10)^2+100)^2} & \frac{\eta}{400^2} & \frac{\eta}{500^2} & \frac{1}{((x-10)^2+100)^2} \\
\frac{\eta}{(x^2+100)^2} & \frac{\eta}{500^2} & \frac{\eta}{400^2} & \frac{\eta}{(x^2+100)^2} \\
\frac{\eta}{(x+10)^4} & \frac{\eta}{500^2} & \frac{\eta}{200^2} & \frac{\eta}{(x+10)^4} \\
\frac{\eta}{(x^2+100)^2} & \frac{\eta}{500^2} & \frac{\eta}{400^2} & \frac{\eta}{(x^2+100)^2} \\
\frac{\eta}{(x^2+100)^2} & \frac{\eta}{100^2} & 0 & \frac{\eta}{(x^2+100)^2}
\end{bmatrix}.$$

Further, the matrix G_R appears in the following form[3]

$$\begin{bmatrix}
\frac{\eta}{400^2} & \frac{\eta}{500^2} & 0 & \frac{\eta}{400^2} \\
\frac{\eta}{500^2} & \frac{\eta}{400^2} & \frac{\eta}{100^2} & \frac{\eta}{500^2} \\
\frac{\eta}{500^2} & \frac{\eta}{200^2} & \frac{\eta}{500^2} & \frac{\eta}{500^2} \\
0 & \frac{\eta}{100^2} & \frac{\eta}{400^2} & 0 \\
\frac{1}{100^2} & 0 & \frac{\eta}{500^2} & \frac{\eta}{100^2} \\
\frac{\eta}{500^2} & \frac{1}{200^2} & \frac{\eta}{500^2} & \frac{\eta}{500^2} \\
\frac{\eta}{100^2} & 0 & \frac{1}{500^2} & \frac{\eta}{100^2} \\
\frac{\eta}{500^2} & \frac{\eta}{400^2} & \frac{\eta}{100^2} & \frac{1}{500^2}
\end{bmatrix}.$$

In this subsection, we compare the results of power optimization problem in both centralized and decentralized cases. We note that in the decentralized case, the power of each node is individually minimized subject to the constraints only applied to the links of the node. The total consumed power is then the sum of per node powers. First, we focus on the centralized case. Fig. 7 shows the curves of optimal total power versus x the position of node A utilizing the centralized power optimization scheme. The figure includes four curves illustrating the optimal power of scenarios (1) through (4) described above.

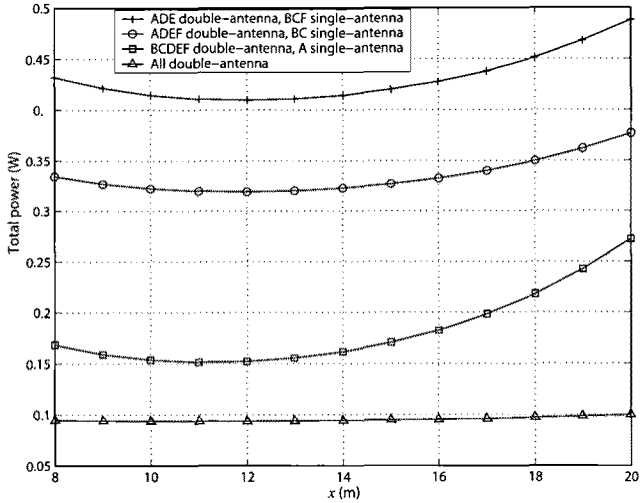

Fig. 7. Centralized optimal curves of total power versus x.

The first interesting observation is the fact that all of the four curves depicted in the figure are in the form of convex curves. While for small values of x interference from other nodes increases total consumed power, for large values of x total consumed power is increased due to the loss of signal strength. The curves show that total consumed powers are at their minimum levels when the value of x represents the position of node A approximately at $x = 12$ m. The main observation when comparing the results of the figure is the fact that the transmission power of a node over a link is reduced if the transmitting and receiving nodes are equipped with a larger number of antennas. As the result, the power consumption of scenarios (1), (2), (3), and (4) are in the descending order.

Next, we focus on the decentralized case and compare its results with those of the centralized case. We argue that the decentralized case provides a practical alternative to the centralized case at the cost of sub-optimality.

Fig. 8 compares the centralized and decentralized curves of total consumed power versus x the position of node A. The nodes are associated with scenarios (1) and (2) described above. As observed from the figure, the results of the decentralized case lead to a lower overall power consumption compared to their centralized counterparts. The results are justified considering the fact that the $SINR$ approximations of the decentralized scheme only take into consideration the interference factors from the nodes within one hop. Since the power components are calculated only with the consideration of local interference factors, they introduce actual inferior measured metrics of QoS. Table 2 illustrates the average measured results of Ψ_i of the associated scenarios in the case of centralized and decentralized schemes. In the decentralized case, per link throughput constraints are equal and sum up to an aggregate throughput

[3]Note that matrix G is represented in the form above merely to adhere to the two-column paper format.

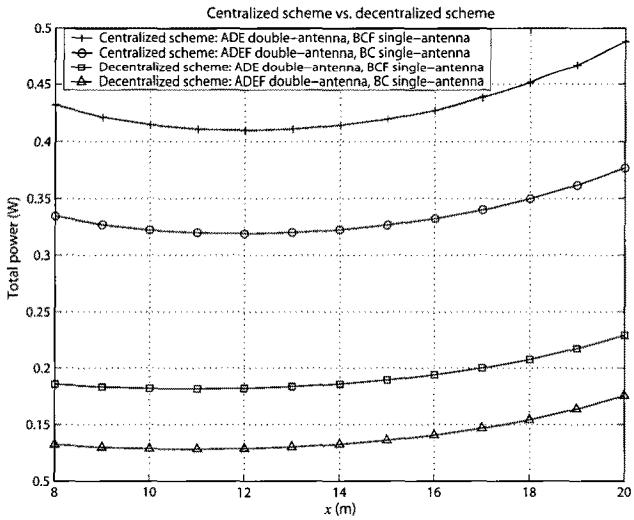

Fig. 8. A comparison of the results of centralized and decentralized power optimization schemes. The curves indicate total optimal consumed power versus x the position of node A.

Table 2. The table of per link average measured results of Ψ_i in the case of centralized (C) and decentralized (D) schemes.

	Link	$\Psi_i\ (C)$	$\Psi_i\ (D)$
Scenario (1)	$\{\mathcal{L}_1, \mathcal{L}_4\}$	0.0050	$[0.0064, 0.0065]$
	$\{\mathcal{L}_2, \mathcal{L}_5\}$	0.0050	$[0.0052, 0.0052]$
	$\{\mathcal{L}_3, \mathcal{L}_6\}$	0.0050	$[0.0057, 0.0058]$
	$\{\mathcal{L}_7, \mathcal{L}_8\}$	0.0050	$[0.0016, 0.0118]$
Scenario (2)	$\{\mathcal{L}_1, \mathcal{L}_4\}$	0.0050	$[0.0064, 0.0064]$
	$\{\mathcal{L}_2, \mathcal{L}_5\}$	0.0050	$[0.0051, 0.0051]$
	$\{\mathcal{L}_3, \mathcal{L}_6\}$	0.0050	$[0.0056, 0.0056]$
	$\{\mathcal{L}_7, \mathcal{L}_8\}$	0.0050	$[0.0096, 0.0096]$

of 2 Mbps. Comparing the results, we observe that while the throughput constraints are always active, the block loss probability difference between centralized and decentralized schemes for scenarios (2) and (5) are in the range of $[3.8\%, 57.6\%]$ and $[1.9\%, 47.9\%]$. The results reveal that the use of the decentralized scheme leads to (1) lower consumed power, (2) higher block loss probability, and (3) less complexity compared to the use of of centralized scheme.

We end this section by commenting on our complexity results. We have observed that an average of 20 and no more than 30 iterations are required for convergence of the centralized algorithm. The numbers in the case of decentralized algorithm are 3 and 5, respectively. Further, we have observed that utilizing a 3-state Markov chain lowers the total consumed power compared to the case of a 2-state Markov chain, at the cost of a higher overhead of calculation.

V. CONCLUSION

In this paper, we examined the problem of resource allocation in Rician and Rayleigh fading wireless ad-hoc networks with temporally correlated loss. We considered accommodating nodes with multiple-transmit multiple-receive antenna systems. We analyzed fading statistics of SINR, an important metric of transmission quality. Relying on exact expressions of symbol error rates for multiple-transmit multiple-receive antenna systems and based on the analysis of fading statistics of SINR, we modeled temporally correlated loss behavior of the fading wireless channel with finite-state Markov chains. Relying on an adaptive modulation scheme derived from exact symbol error rate expressions, we optimized the aggregate throughput and the overall transmission power subject to loss and other constraints. We also numerically presented our results for sample ad-hoc networks under slow fading assumption.

REFERENCES

[1] E. N. Gilbert, "Capacity of a burst-noise channel," *Bell Syst. Tech. J.*, Sept. 1960.

[2] E. O. Elliott, "Estimates on error rates for codes on burst-noise channels," *Bell Syst. Tech. J.*, Sept. 1963.

[3] F. Swarts and H. C. Ferreira, "Markov characterization of channels with soft decision outputs," *IEEE Trans. Commun.*, May 1993.

[4] H. S. Wang and N. Moayeri, "Finite-state markov channel: A useful model for radio communications channels," *IEEE Trans. Veh. Technol.*, Feb. 1995.

[5] C. C. Tan and N. C. Beaulieu, "On first-order markov modeling for the Rayleigh fading channel," *IEEE Trans. Commun.*, Dec. 2000.

[6] S. M. Alamouti, "A simple transmitter diversity scheme for wireless communications," *IEEE J. Sel. Areas Commun.*, Nov. 1998.

[7] V. Tarokh, H. Jafarkhani, and A. R. Calderbank, "Space-time block coding from orthogonal designs," *IEEE Trans. Inf. Theory*, July 1999.

[8] M. Andersin, Z. Rosberg, and J. Zander, "Gradual removals in cellular PCS with constrained power control and noise," *IEEE/ACM Trans. Netw.*, Apr. 1997.

[9] N. Bambos, S. Chen, and G. Pottie, "Radio link admission algorithms for wireless networks with power control and active link quality protection," in *Proc. IEEE INFOCOM*, 1995.

[10] S. Ulukus and R. Yates, "Adaptive power control and MMSE interference suppression," *ACM/Baltzer Wireless Netw.*, 1998.

[11] M. Chiang, D. O'Neil, D. Julian, and S. Boyd, "Resource allocation for QoS provisioning in wireless ad hoc networks," in *Proc. IEEE GLOBE COM*, 2001.

[12] S. Kandukuri and S. Boyd, "Optimal power control in interference limited fading wireless channels with outage probability specifications," *IEEE J. Sel. Areas Commun.*, 2002.

[13] M. Hayajneh and C. T. Abdallah, "Performance of game theoretic power control algorithms for wireless data in fading channels," in *Proc. IEEE GLOBECOM*, 2003.

[14] M. J. Shah and P. G. Flikkema, "Power-based leader selection in ad-hoc wireless networks," *IEEE Int. Performance, Comput. Commun. Conf.*, 1999.

[15] R. Ramanathan and R. Rosales-Hain, "Topology control of multihop wireless networks using transmit power adjustment," in *Proc. IEEE INFO COM*, 2000.

[16] H. Mahdavi-Doost, M. Ebrahimi, and A. K. Khandani, "Characterization of SINR region for interfering links with constrained power," *IEEE Trans. Inf. Theory*, June 2010.

[17] E. Matskani, N. D. Sidiropoulos, Z. Q. Luo, and L. Tassiulas, "Convex approximation techniques for joint multiuser downlink beamforming and admission control," *IEEE Trans. Wireless Commun.*, July 2008.

[18] D. Catrein and R. Mathar, "Segregating in- and other-cell interference with applications to decentralized admission control," *IEEE Trans. Commun.*, Aug. 2009.

[19] M. Chiang, W. T. Chee, D. P. Palomar, D. O'Neill, and D. Julian, "Power control by geometric programming," *IEEE Trans. Wireless Commun.*, July 2007.

[20] G. Zheng, K. K. Wong, and T. S. Ng, "Energy-efficient multiuser SIMO: Achieving probabilistic robustness with Gaussian channel uncertainty," *IEEE Trans. Wireless Commun.*, June 2009.

[21] A. Papoulis and S. U. Pillai, *Probability, Random Variables, and Stochastic Processes, 4th ed.* McGraw-Hill, 2002.

[22] A. A. Abu-Dayya and N. C. Beaulieu, "Switched diversity on microcellular Ricean channels," *IEEE Trans. Veh. Technol.*, Nov. 1994.

[23] D. A. Zogas and G. K. Karagiannidis, "Infinite-series representations associated with the bivariate Rician distribution and their applications," *IEEE Trans. Commun.*, Nov. 2005.

[24] N. C. Beaulieu and K. T. Hemachandra, "New simple solutions for the bivariate Rician PDF and CDF," in *Proc. IEEE WCNC*, 2010.
[25] M. O. Hasna, M. S. Alouini, and M. K. Simon, "Effect of fading correlation on the outage probability of cellular mobile radio systems," in *Proc. IEEE VTC*, 2001.
[26] H. Jafarkhani, P. Ligdas, and N. Farvardin, "Adaptive rate allocation in a joint source-channel coding framework for wireless channels," in *Proc. IEEE VTC*, 1996.
[27] H. Yousefi'zadeh, H. Jafarkhani, and F. Etemadi, "Progressive image transmission over noisy channels: An end-to-end statistical optimization framework," *IEEE JSTSP*, Apr. 2008.
[28] M. K. Simon and M. S. Alouini, *Digital Communication over Fading Channels: A Unified Approach to Performance Analysis.* John Wiley, 2000.
[29] H. Jafarkhani, *Space-Time Coding: Theory and Practice.* Cambridge University Press, 2005.
[30] D. P. Bertsekas, *Nonlinear Programming, 2nd ed.* Athena Scientific Publishing, 1999.
[31] D. F. Shanno, "Conditioning of quasi-newton methods for function minimization," *Mathematics of Comput.*, vol. 24, 1970.
[32] K. Chawla and X. Qiu, "Throughput performance of adaptive modulation in cellular systems," in *Proc. IEEE Conf. Universal Pers. Commun.*, 1998.
[33] S. T. Chung and A. J. Goldsmith, "Degrees of freedom in adaptive modulation: A unified view," *IEEE Trans. Commun.*, Sept. 2001.
[34] W. C. Jakes, *Microwave Mobile Communications.* John Wiley Publishing, 1994.
[35] V. Tarokh, H. Jafarkhani, and A. R. Calderbank, "Space-time block coding for wireless communications: Performance results," *IEEE J. Sel. Areas Commun.*, Mar. 1999.
[36] H. Yousefi'zadeh, H. Jafarkhani, and M. Moshfeghi, "Power optimization of wireless media systems with space-time block codes," *IEEE Trans. Image Process.*, July 2004.

Homayoun Yousefi'zadeh received the B.S. degree from Sharif University of Technology, the M.S. degree from Amirkabir University of Technology, and the Ph.D. degree from University of Southern California, Los Angeles, all in Electrical Engineering, in 1989, 1993, and 1997, respectively. He is currently an Associate Adjunct Professor in the Department of Electrical Engineering and Computer Science at the University of California, Irvine. He is also a Consulting Scientist at the Boeing company. Most recently, he was the CTO of TierFleet, Inc. working on distributed database systems, a senior technical, and business manager at Procom Technology focusing on storage networking, and a Technical Consultant at NEC Electronics designing and implementing distributed client-server systems. He is the inventor of four patents. In the past, he served as the Chairperson of the systems' management workgroup of the Storage Networking Industry Association (SNIA), and a Member of the scientific advisory board of the Integrated Media Services Center (IMSC) at the University of Southern of California. He is an Editor of the IEEE Transactions on Wireless Communications and an Editor of the KICS/IEEE Journal of Communications and Networks (JCN). From 2005 to 2010, he was an Associate Editor of the IEEE Communications Letters. From 2006 to 2010, he was an Editor of the IEEE Wireless Communications Magazine. He also served as the Lead Guest Editor of the IEEE Journal of Special Topics in Signal Processing (JSTSP) the issue of April 2008. He serves regularly as a Member of the Technical Program Committees of various IEEE COMSOC conferences including ICC, GLOBECOM, and WCNC. He is a Senior Member of the IEEE and a recipient of JCN 2009 Best Paper Award.

Hamid Jafarkhani received the B.S. degree in electronics from Tehran University in 1989 and the M.S. and Ph.D. degrees both in Electrical Engineering from the University of Maryland at College Park in 1994 and 1997, respectively. In 1997, he was a Senior Technical Staff Member at AT&T Labs-Research and was later promoted to a Principal Technical Staff Member. He is currently a Chancellor's Professor at the Department of Electrical Engineering and Computer Science, University of California, Irvine, where he is also the Director of Center for Pervasive Communications and Computing. He ranked first in the nationwide entrance examination of Iranian universities in 1984. He was a co-recipient of the American Division Award of the 1995 Texas Instruments DSP Solutions Challenge. He received the best paper award of ISWC in 2002 and an NSF Career Award in 2003. He received the UCI Distinguished Mid-Career Faculty Award for Research in 2006 and the School of Engineering Fariborz Maseeh Best Faculty Research Award in 2007. Also, he was a co-recipient of the 2006 IEEE Marconi Best Paper Award in Wireless Communications and the 2009 best paper award of the Journal of Communications and Networks.

He was an Associate Editor for IEEE Communications Letters from 2001-2005, an Editor for the IEEE Transactions on Wireless Communications from 2002-2007, an Editor for the IEEE Transactions on Communications from 2005-2007, and a Guest Editor of the special issue on "MIMO-optimized transmission systems for delivering data and rich content" for the IEEE Journal of Selected Topics in Signal Processing in 2008. Currently, he is an Area Editor for the IEEE Transactions on Wireless Communications. He is listed as a highly cited researcher in http://www.isihighlycited.com. According to the Thomson Scientific, he is one of the top 10 most-cited researchers in the field of "computer science" during 1997-2007. He is an IEEE Fellow and the author of the book "Space-Time Coding: Theory and Practice."